Novel Hot Spot Mitigation Technique to Enhance Photovoltaic Solar Panels Output Power Performance

Mahmoud Dhimish, Violeta Holmes, Peter Mather, & Martin Sibley

School of Computing and Engineering, University of Huddersfield, United Kingdom

Abstract

Hot spotting is a reliability problem in photovoltaic (PV) panels where a mismatched cell heats up significantly and degrades PV panel output power performance. High PV cell temperature due to hot spotting can damage the cell encapsulate and lead to second breakdown, where both cause permanent damage to the PV panel. Therefore, the design and development of a hot spot mitigation technique is proposed using a simple, low-cost and reliable hot spot activation technique. The hot spots in the examined PV system is detected using FLIR i5 thermal imaging camera.

Several experiments have been studied during various environmental conditions, where the PV module P-V curve was evaluated in each observed test to analyze the output power performance before and after the activation of the proposed hot spot mitigation technique. One PV module affected by hot spot was tested. The output power increased by approximate to 3.6 W after the activation of the hot spot mitigation technique. Additional test has been carried out while connecting the hot spot PV module in series with two other PV panels. The results indicate that there is an increase of 3.57 W in the output power after activating the hot spot mitigation technique.

Keywords: Hot spot protection, photovoltaic (PV) hot spotting analysis, solar cells, thermal imaging

1. Introduction

Photovoltaic (PV) hot spots are a well-known phenomenon, described as early as in 1969 [1] and still present in PV modules [2 and 3]. PV hot spots occur when a cell, or group of cells, operates at reverse-bias, dissipating power instead of delivering it and, therefore, operating at abnormally high temperatures. This increase in the cells temperature will gradually degrade the output power generated by the PV module as explained by M. Simon & L. Meyer [4].

Hot spots are relatively frequent in current PV modules and this situation will likely persist as the PV module technology is evolving to thinner wafers, which are prone to developing micro-cracks during the manipulation process such as manufacturing, transportation and installation [5 and 6].

PV hot spots can be easily detected using IR inspection, which has become a common practice in current PV applications as shown in [7]. However, the impact of hot spots on operational efficiency and PV lifetime have been scarcely addressed, which helps to explain why there is lack of widely accepted procedures which deals with hot spots in practice as well as specific criteria referring to acceptance or rejection of affected PV module in commercial frameworks as described by R. Moretón et al [8].

In the past, the increase in the number of bypass diodes (up to one diode for each cell) has been proposed as a possible solution [9 and 10]. However, this approach has not encountered the favor of crystalline PV modules producers since it requires a not negligible technological cost and can be even detrimental in terms of power production when many diodes are activated because of their power consumption as discussed by S. Daliento et al [11].

In addition, the main prevention method for hot spotting is a passive bypass diode that is placed in parallel with a string of PV cells. The use of bypass diodes across PV strings is standard practice that is required in crystalline silicon PV panels [12 and 13]. Their purpose is to prevent hot spot damage that can occur in series-connected PV cells [14]. Bypass diodes turn "on" to provide an alternative current path and attempt to prevent extreme reverse voltage bias on PV strings. The general misconception is that bypassing a string protects cells against hot spotting.

More recently, it has been shown that the distributed MPPT approach suggested by M. Coppola [15] is beneficial for mitigating the hot spot in partially shaded modules with a temperature reduction up to 20 ^{0}C for small shadows. On the other hand, [16 and 17] showing the "inadequateness" of the standard bypass diode, the insertion of a series-connected switch are suited to interrupt the current flow during bypass activation process. However, this solution requires a quite complex electronic board design that needs devised power supply and suitable control logic for activation the hot spot mitigation technique.

A modified bypass circuit for improving the hot spot reliability of solar panels is proposed by S, Daliento [18]. The technique relies on series-connected power MOSFET that subtracts part of the reverse voltage from the shaded solar cell, thereby acting as a voltage divider, while the bypass circuit does not require either a control logic or power supply and can be subtitled to the standard bypass diodes of the PV panels.

This paper presents a simple solution for mitigating the impact of hot spots on solar cells. The presented hot spot mitigation technique consists of two MOSTEFs connected to the PV panel which has been affected by a hot spot. Several experiments have been studied during various environmental conditions, where the PV module P-V curve was evaluated in each observed test to analyze the output power performance before and after the activation of the proposed hot spot protection technique.

One PV module affected by a hot spot was tested. The output power increased by approximate to 3.6 W after the activation of the hot spot mitigation technique. Additional test has been examined while connecting the hot spot PV module in series with two other PV panels. The results indicate that there is an increase in the output power approximately equals to 3.57 W after activating the hot spot mitigation technique.

This paper is organized as follows: section 2 illustrates the examined PV module electrical characteristics, while section 3 describes the proposed hot mitigation technique. Section 4 shows the validation process of the proposed hot spot protection method using two case studies. A brief discussion using conventional bypass diodes, PV cells with low reverse-breakdown voltage and active bypass diodes are compared with the proposed hot spot mitigation technique in section 4. Lastly, section 5 demonstrates the conclusion of the entire work.

2.   *Examined Photovoltaic Module Characteristics*

The PV system used in this work comprises a PV plant containing 9 polycrystalline silicon PV modules each with a nominal power of 220 Wp. The photovoltaic modules are organized in 3 strings and each string is made up of 3 series-connected PV modules. Using a photovoltaic connection unit which is used to enable or disable the connection of any PV modules from the entire PV plant, each photovoltaic string is connected to a Maximum Power Point Tracker (MPPT) which has an output efficiency not less than 98.5% [19 and 20]. The existing PV system is shown in Fig. 1.

SMT6 (60) P solar module manufactured by Romag has been used in this work. The tilt angle of the PV installation is 42º. The electrical characteristics of the solar module are shown in Table 1. Additionally, the standard test conditions (STC) for the solar panels are: solar irradiance (G): 1000 W/m^2 and PV module temperature (T): 25 °C.

Fig. 1. Examined PV system installed at the University of Huddersfield, United Kingdom

Table 1 PV module electrical characteristics

PV module electrical characteristics	Value
PV peak power	220 W
One PV cell peak power	3.6 W
Voltage at maximum power point (V_{mpp})	28.7 V
Current at maximum power point (I_{mpp})	7.67 A
Open Circuit Voltage (V_{oc})	36.74 V
Short Circuit Current (I_{sc})	8.24 A
Number of cells connected in series	60

3.   *Hot Spot Detection and Protection System*

Thermal imaging technique is one of the most common techniques to detect hot spots in PV modules. Another hot spot detection method proposed by K. Kim et al [23] uses the impedance of the PV string to detect hot spotting conditions. A distinct change is observed in substring impedance parameters when partial shading occurs, thus, this technique does not need a thermal image. However, it require to measure the impedance of the PV module frequently using complex algorithms.

In this paper, the detection of the hot spots are captured using FLIR i5 thermal imaging camera which nearly costs £550. The camera specification is presented in Table 2 [21]. After inspecting the examined PV system using the thermal camera, one hot spot was detected in the fifth PV module as shown in Fig. 2(a).

Once hot spot is detected, open circuiting the substring that contains the mismatched cell is a guaranteed method to prevent hot spotting because no current or power will flow through any cell in the PV substring. When the PV module is bypassed, it produces no net output power. Since the affected substring contribution is zero is such an event, why not open-circuit the PV module to protect it from hot spotting.

The proposed hot spot protection system is shown in Fig. 2(b). Switch 1 is in series with the PV module is normally "on"; it opens when a hot spot condition is detected to prevent further hot spot mitigation technique. Switch 2 is in parallel with the PV module and is normally "off"; it turn "on" to allow a bypass current path when the PV string is open circuited. The two switch PV mitigation technique has been implemented and connected to the PV panel which contains the hot spot.

As can be noticed, the proposed technique is simple to implement, since it requires only to add additional MOSFETs to the PV panel. The basic implementation of the proposed hot spot mitigation technique using MOSFETs is shown in Fig. 2(c).

The MOSFETs were controlled using a microcontroller "16F877A". Switch 2 is activated every 3 hour for 2 minutes. This is acknowledged by the hot spot protection mode. The activation interval (2 minutes) was selected based on the analysis of thermal images, which will be shown in next section.

One of the biggest challenge was to decide how often it is require to mitigate the hot spotted solar cell using the activation of the hot spot protection mode. After an extensive experiments, we have found that 3 hours is the maximum acceptable duration before the hot spot reappears again in the PV solar cell. Brief analysis is shown in the next section, Figs. 5(a) and 6.
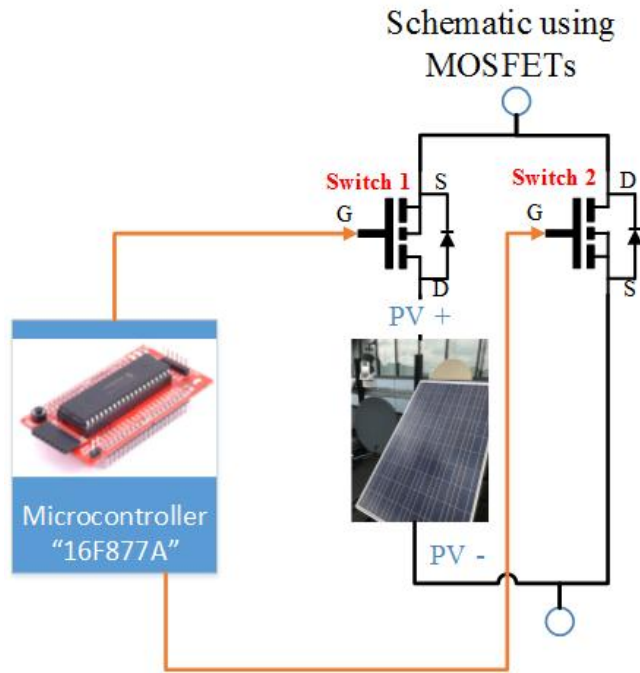
Table 1 FLIR i5 camera specification

Comparison	Value
Thermal image quality	100x100 pixels
Field of view	21^0 (H) x 21^0 (V)
Thermal sensitivity	32.18 F
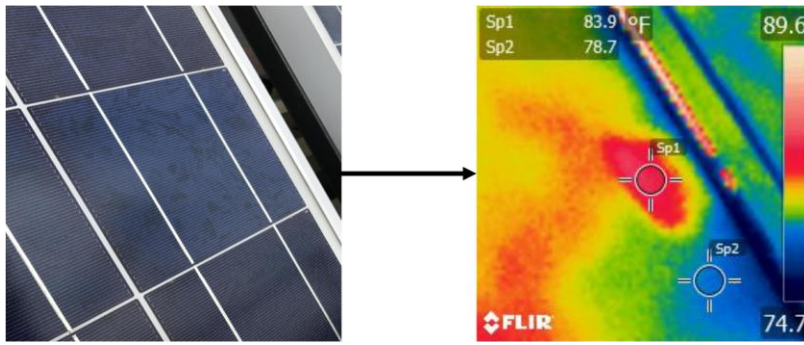
(a)
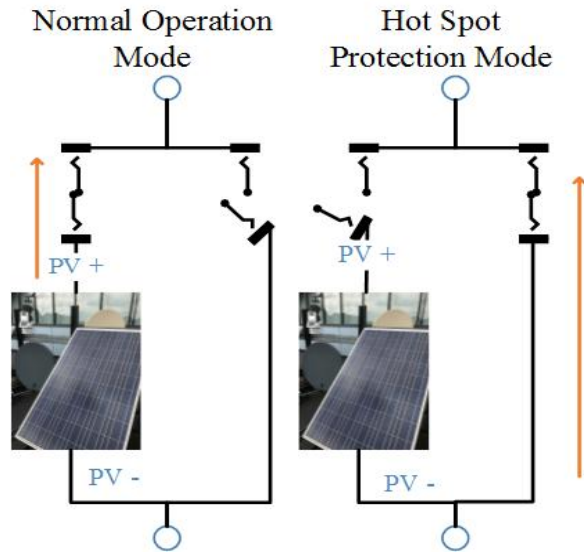
(b)

(c)

Fig. 2. (a) Hot Spot detection using FLIR thermal imaging camera, (b) Hot spot mitigation technique switch states in normal operation mode and hot spot protection mode, (c) Device schematic using MOSFETs

4. Validation of the Proposed Hot Spot Mitigation Technique

4.1 Photovoltaic Hot Spot and P-V Curve Analysis

The proposed hot spot mitigation technique was tested in an experimental setup with a resistive load powered by the PV module which contains the hot spot as shown previously in Fig. 2(a), where the MOSFETs are placed in the PV module as shown in Fig. 2(c).

There are several stages that are used during the operation of the proposed hot spot mitigation technique. These stages are illustrated as the following:

1. Stage 1: when the spot mitigation technique is at start point (before activating the hot spot mitigation technique) the hot spot solar cell has a temperature equals to 83.9 ^{0}F. In addition, the temperature (reference temperature) of the surrounding PV cells are equal to 78.7 ^{0}F. Output thermal image for stage 1 is presented in Fig. 3(a)

2. Stages 2-6: In these stages the hot spot mitigation technique is active (hot spot protection mode). Each stage has been monitored at a time interval equals to 10 seconds. Stages 2-6 are shown in Fig. 3(b-f) respectively, where the hot spot temperature has a large drop in its value at each stage

3. Stage 7: during the operation of the hot spot mitigation technique, after the 6th stage, the solar cell affected by the hot spot has a low drop in its temperature value. Therefore, stage 7 has been captured after 1 min as shown in Fig. 3(g). The minimum value of the temperature is equal to 78.9 ^{0}F, where this value kept the same during the operational process of the hot spot mitigation technique

As can be noticed, the PV solar cell affected by a hot spot has a reduction in its temperature due to the impact of the hot spot mitigation technique applied in the PV module. The difference between the hot spot temperature and the reference solar cell temperature (78.7 ^{0}F) are shown in Table 3. At stage 1, the difference in the temperature is equal to 5.2 ^{0}F. Furthermore, the last stage (after 110 seconds of operation) the difference in the temperature is equal to 0.2 ^{0}F.

After activating the hot spot mitigation technique, the PV module does not contain anymore the hot spot detected previously at stage 1 as can be seen in Fig. 3(h).

Table 3 PV hot spot mitigation technique – output examined stages

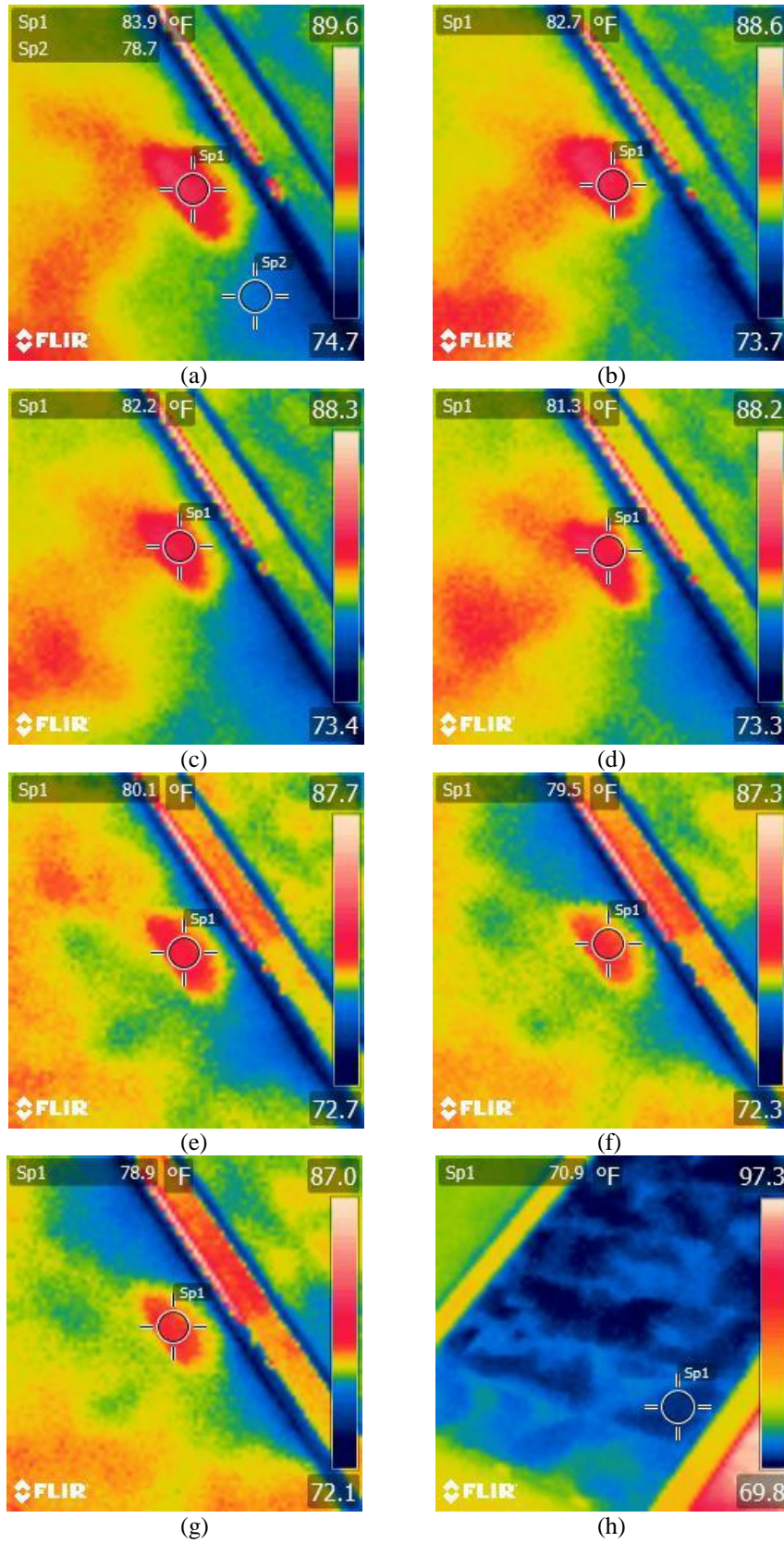| Stage number	Duration (s)	Hot spot temperature (^{0}F)	Difference = hot spot temperature - reference solar cell temperature (^{0}F)
1	0	83.9	83.9 – 78.7 = 5.2
2	10	82.7	82.7 - 78.7 = 4.0
3	20	81.9	82.2 - 78.7 = 3.5
4	30	81.3	81.3 - 78.7 = 2.6
5	40	80.1	80.1 - 78.7 = 1.4
6	50	79.5	79.5 - 78.7 = 0.8
7	110	78.9	78.9 - 78.7 = 0.2

Fig. 3. PV module infrared images after considering the PV hot spot mitigation technique. (a) Stage 1-at time=0s, (b) Stage 2-at time=10s, (c) Stage 3-at time=20s, (d) Stage 4-at time=30s, (e) Stage 5-at time=40s, (f) Stage 6-at time=50s, (g) Stage 7-at time=110s, (h) PV module does not contain anymore the detected hot spot

7

The main reason of the hot spot mitigation technique is to improve the PV module output power. Therefore, the value of the power with and without the proposed technique was monitored in two different irradiance levels (G: 835 and 612 W/m^2) and evaluated using the P-V curve.

Fig. 4(a) shows the output P-V curve of the PV module at G: 835 W/m^2. The output power without the hot spot mitigation technique is equal to 177.2 W, however, during the same environmental conditions, the hot spot mitigation technique was activated. The output power with the hot spot mitigation technique is equal to 180.8 W. There is an increase in the output measured power equals to 3.6 W after the activation of the hot spot mitigation technique.

Another experimental condition is examined under G: 612 W/m^2. The output P-V curve is shown in Fig. 4(b). The measured output power with and without using the hot spot mitigation technique are equal to 129.22 W and 125.59 W respectively. Where the PV module output power enhancement using the hot spot mitigation technique is equal to 3.63 W.

In both experiments, when the status of the MOSFETs are ON, their conduction resistance (Rds (on)) creates additional losses. Thus, it will drop the measured power/voltage. This loss will be further explained in section 4.4.
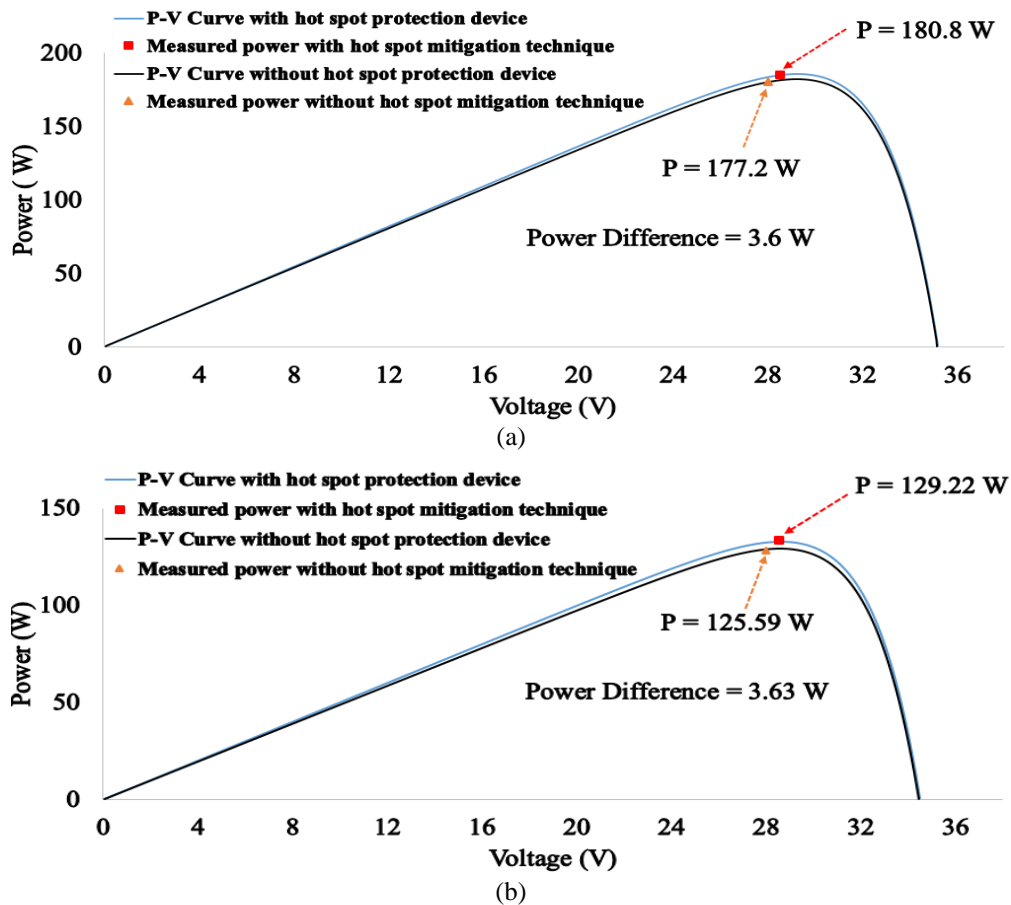

(a)

(b)

Fig. 4. Photovoltaic P-V curve. (a) With and without the considering hot spot mitigation technique at G: 835 W/m^2, (b) With and without the considering hot spot mitigation technique at G: 612 W/m^2

8

4.2   *Evaluating the Hot Spot Mitigation Technique Using a Full Day Experimental Data*

In order to judge the appropriateness of the proposed hot spot mitigation technique, the evaluation of the PV module with and without the mitigation technique was assessed.

Fig. 5(a) shows the measured PV power. As can be seen, the mitigation technique is activated every 3 hours, each lasts for 2 minutes, and therefore in this period the output measured power generated from the PV module is zero. However, the PV module is back at its optimum power level when switching "off" the hot spot protection mode. The average power without and with the hot spot mitigation technique is equal to 73.6 W_p and 76.4 W_p respectively. Thus, the average increase in the PV generated power for a period of full day is equal to 2.8 W_p.

Fig. 5(b) shows the cumulative energy of the PV module with and without the hot spot mitigation technique. The cumulative energy of the PV module without the hot spot mitigation technique equals to 1.12 kWh, however, there is an increase of 0.03 kWh after using the hot spot mitigation technique.

Fig. 5(c) shows a statistical linear regression analysis of the power loss for both PV measured data, the power loss is measured with respect to the theoretical MPP. This figure verifies that there is a huge reduction in the output measured power for a hot spotted PV module especially in high irradiance conditions. Using the hot spot mitigation technique this huge reduction dropped significantly to a suitable level.
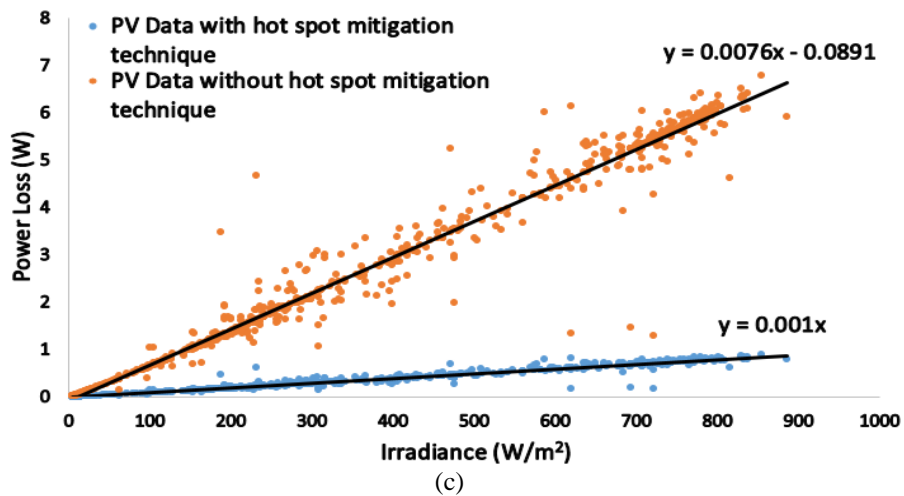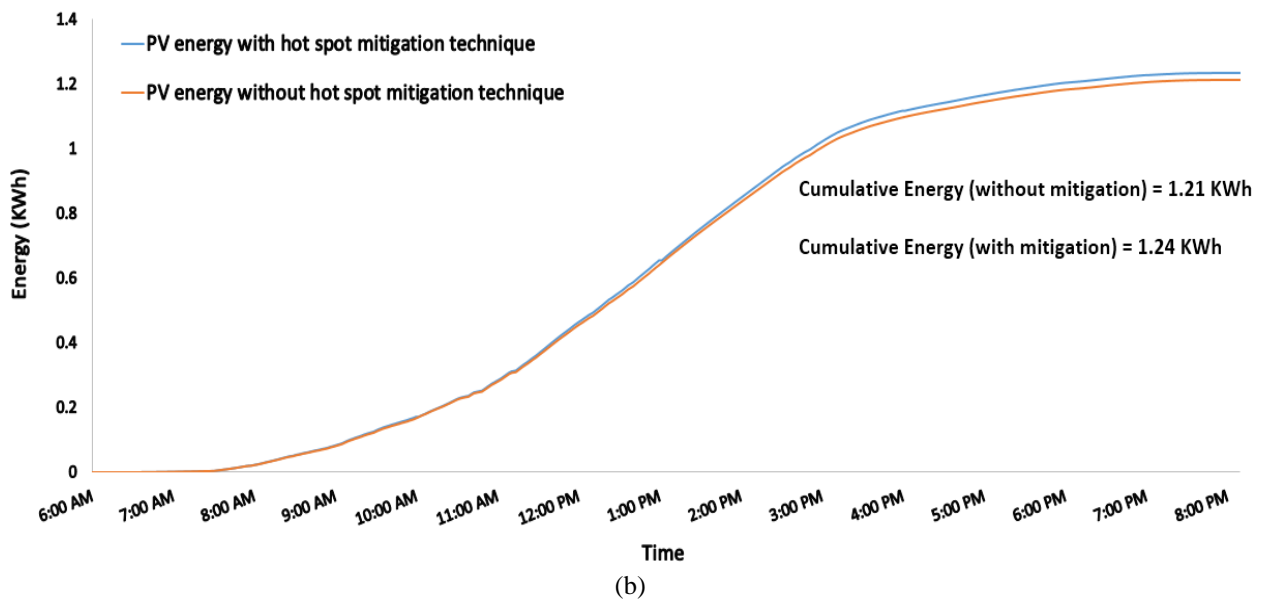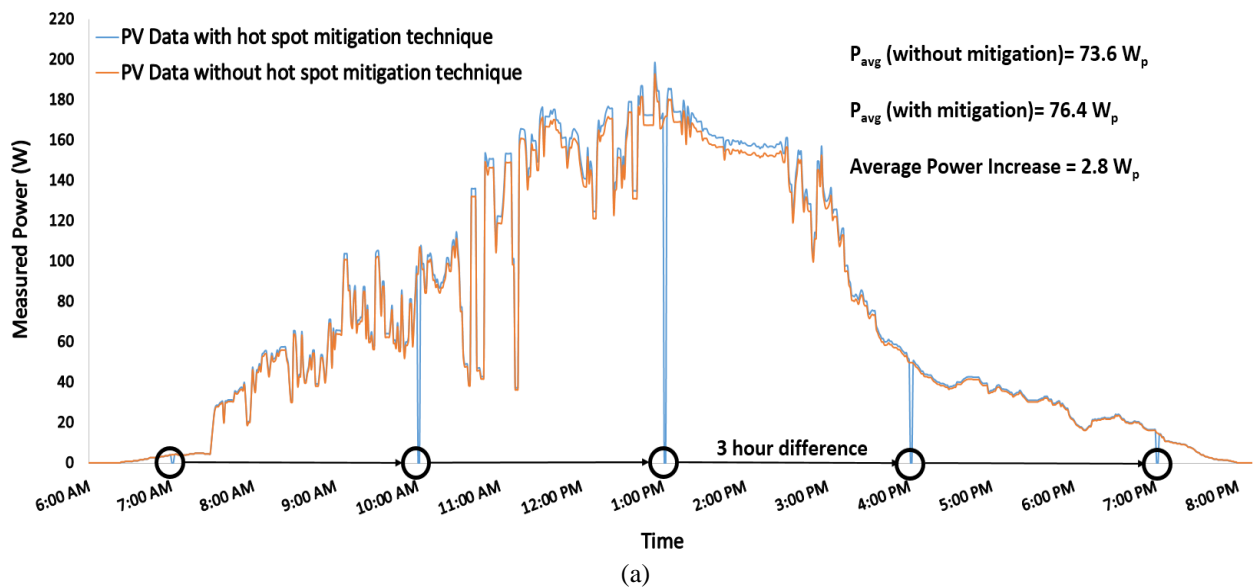
Fig. 5. (a) Measured PV output power, (b) PV cumulative energy, (c) Statistical linear regression for PV output power loss

As shown in Fig. 5(a), the hot spot mitigation technique is activated every 3 hours, for 2 minutes. This time period was selected based on the hot spot temperature. Fig. 6 shows the hot spot vs. adjacent solar cells temperature after 1, 2, and 3 hours of activating the hot spot protection mode.

As can be noticed, the difference in the temperature raises during the time, since there is no mitigating technique applied to mitigate the hot spot temperature.

In the last case (After 3 hours of activating the hot spot protection mode) the PV hot spot temperature is equal to 78.3 ^{0}F, whereas the adjacent PV solar cells temperature is around 73.0 ^{0}F. Therefore, the difference in the temperature is equal to 5.3 ^{0}F.

According to the results shown previously in Table 3, the maximum difference between the hot spot and the adjacent PV solar cells is around 5.2 ^{0}F, which is approximately equal to the maximum difference of the temperature obtained after 3 hours of activating the hot spot protection mode shown in Fig. 6. Therefore, the time period of 3 hours will be chosen as a threshold to control the proposed hot spot mitigation technique, hence that is the worst-case scenario to mitigate the hot spot in the PV module.
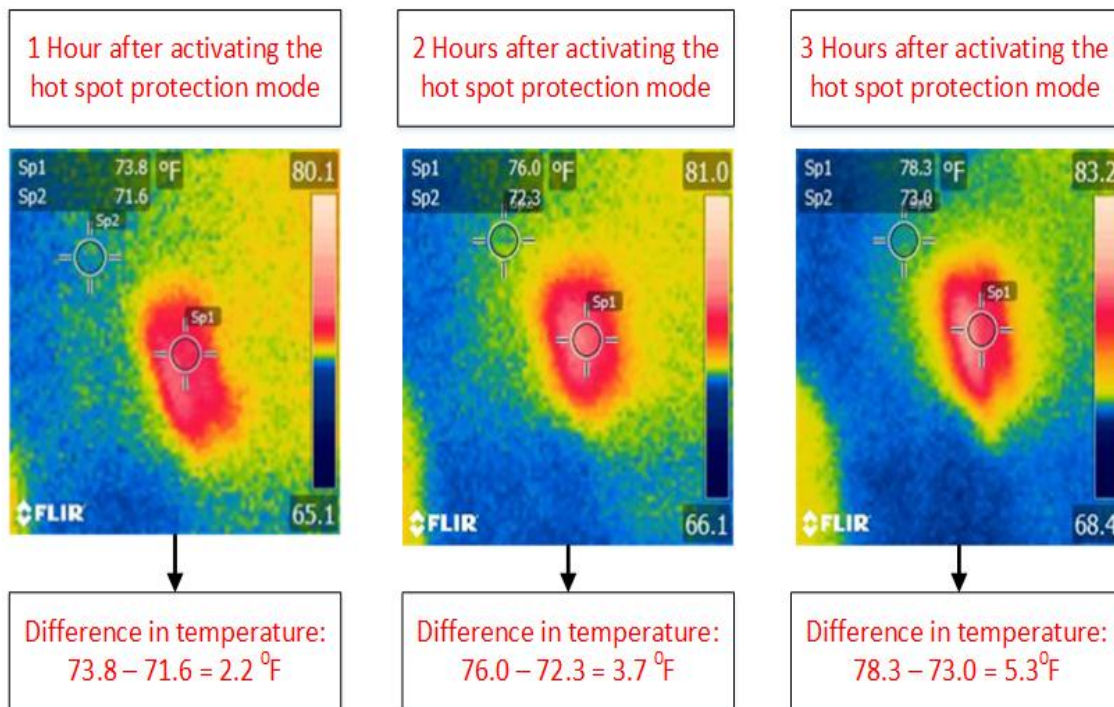

Fig. 6 The hot spot temperature after 1, 2, and 3 hours of activating the hot spot protection mode

4.3   *Evaluating the Hot Spot Mitigation Technique Using a String of PV Modules*

In this section, the proposed hot protection mitigation technique will be activated while connecting the PV module which is affected by the hot spot in series with two PV modules as shown in Fig. 7. In addition, in order to examine the behavior of the tested PV modules, a P-V curve tracer [22] was used because the solar irradiance and PV ambient temperature play a major role in shaping the P-V curve for each tested PV module.

Fig. 7 shows that the P-V curve tracer has thee output P-V curves. Where P-V curve 1 is associated to the hot spotted PV module.

Moreover, as stated in section 4.1, the period for activating the hot spot mitigation technique is equal to 2 minutes. This short period ensures that the P-V curves and measured output power for each examined PV module do not change rapidly due to the impact of the thermal effect of the PV module which are not directly related to the hot spot itself.

Fig. 8(a) show the P-V curves for each examined PV module with and without the hot spot mitigation technique. As can be seen, the second and third PV modules which are presented by P-V curve 2 and P-V curve 3 respectively, does not change. However, the P-V curve 1 changes after the activation of the hot spot mitigation technique.

The output power with activating the mitigation technique for the hot spotted PV module is equal to 164.39 W, while without activating the hot mitigation technique, the output power is equal to 160.85 W. Furthermore, Fig. 8(b) show the P-V curves with and without the activation of the hot spot mitigation technique for the examined series PV system. The total increase of the measured power is equal to 3.57 W.
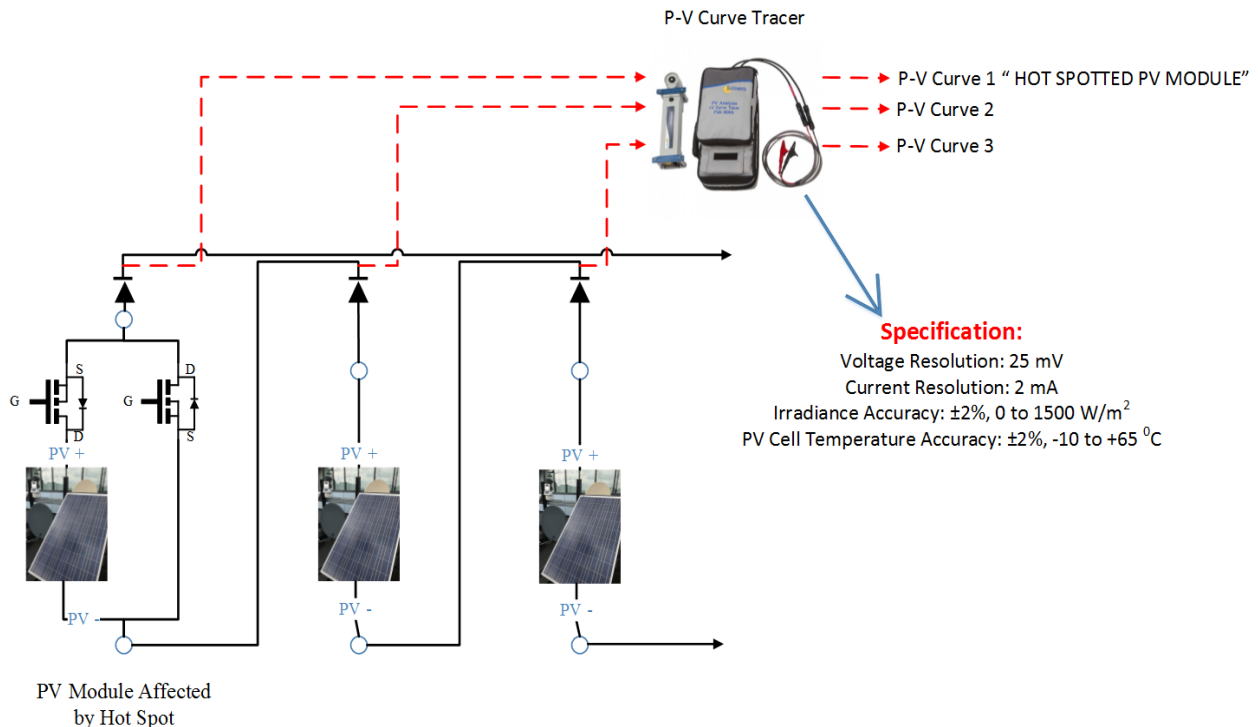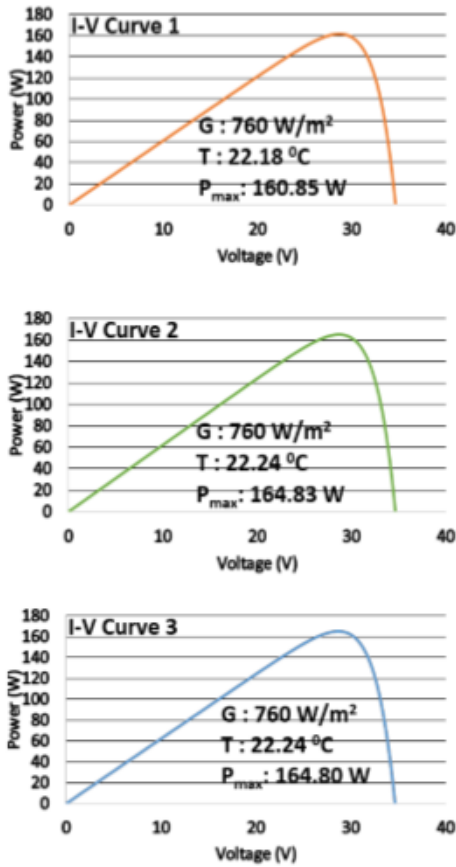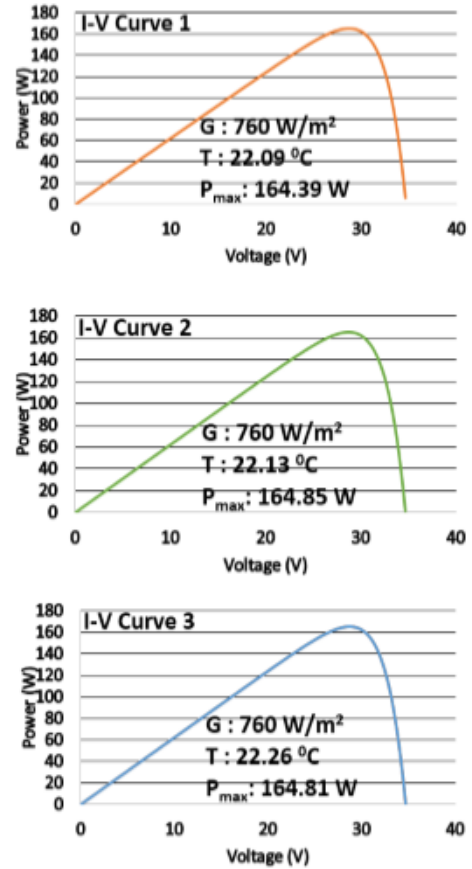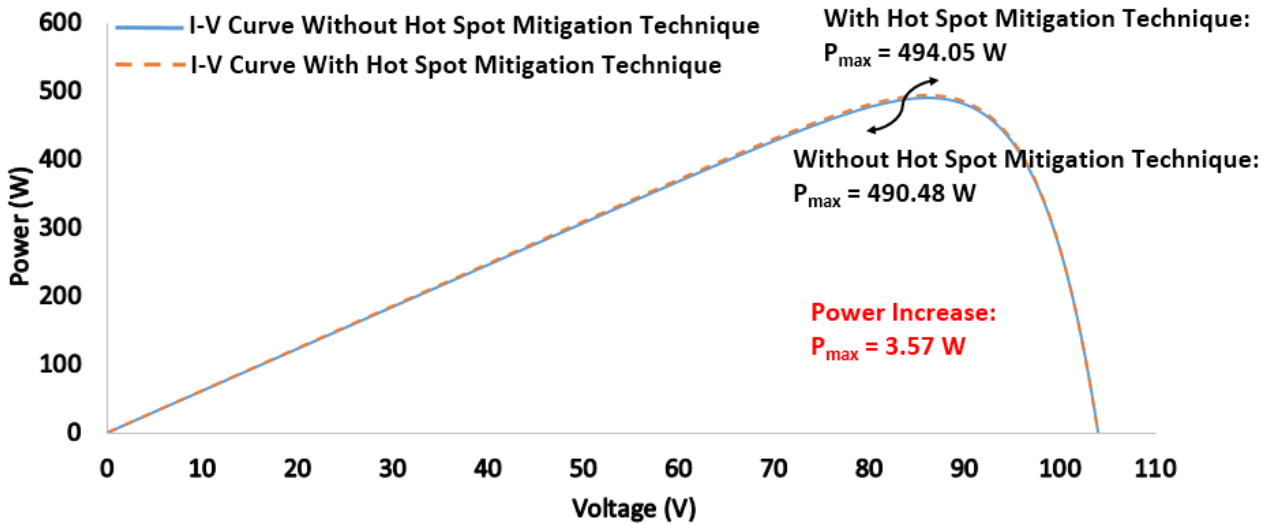

Fig. 7. Examined PV String Connection

(a)

(b)

Fig. 8. (a) P-V curves for the tested PV modules under solar irradiance 760 W/m², (b) P-V curve for the PV system with and without the activation of the hot spot mitigation technique

4.4   Analysis of the Series Resistance for the Proposed Hot Spot Mitigation Technique

When the MOSFETs are ON, their conduction resistance ($R_{ds\ (on)}$) creates additional losses. Therefore, it is extremely important to select for the hot spot mitigation technique a suitable MOSFET which has low $R_{ds\ (on)}$.

Fig. 9(a) show the theoretical circuit diagram of a PV module. The PV module has an extra conduction resistance due to the MOSFET connection which is described in Fig. 9(b).

In this work, IRFP260NPBF MOSFET Transistor has been used, where the $R_{ds\ (on)}$ is equal to 40 mΩ. The cost of this transistor is approximate to £2.15. Moreover, image of the MOSFET is shown in Fig. 9(c).

Due to the additional conduction loss of the MOSFET, the I-V curve under STC has been conducted for the examined PV module. Fig. 10 proves that the maximum power without MOSFET under STC is equal to 220 W. However, after the connection of the MOSFET, the maximum power is equal to 219.72W, thus the power loss is 0.28 W per PV module.

This loss is very small compared to the measured power loss of a hot spotted PV module which is found to be 3.6 W. Therefore, this technique provides a simple and reliable solution to mitigate hot spots in PV plants. In addition, the mitigation technique including MOSFETs can only be added to the hot spotted PV modules. However, it is required to localize the hot spotted PV modules using thermal image technique or any other suitable method.
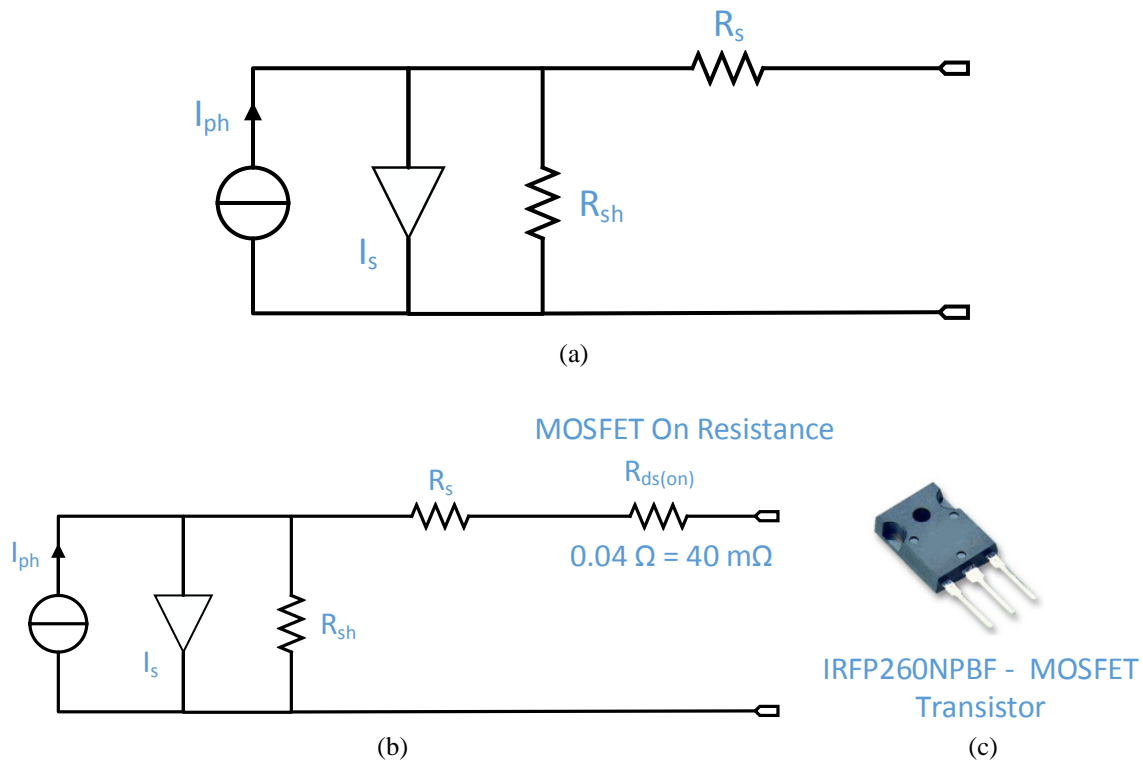

Fig. 9. (a) PV module circuit diagram without proposed hot spot mitigation technique, (b) PV module circuit diagram with hot spot mitigation technique, (c) MOSFET used in this work
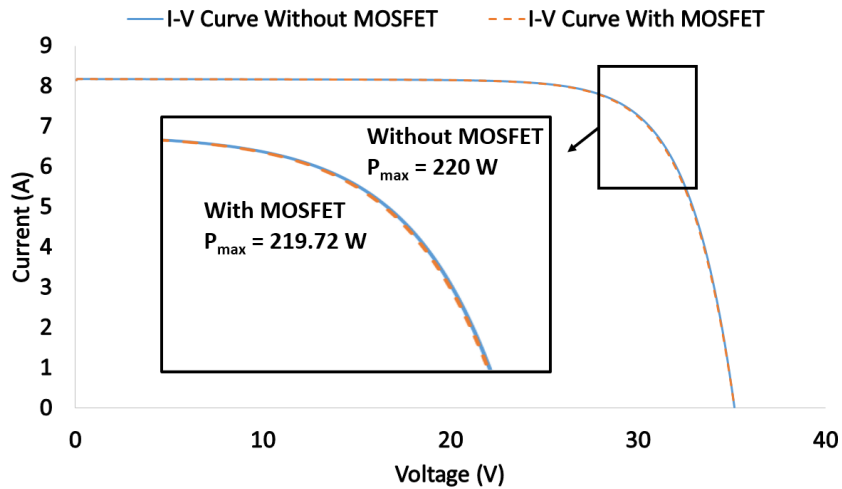
Fig. 10. PV module I-V curve with and without MOSFET

5.   *Discussion*

In addition to the widely used hot spot protection method of bypass diodes, recent developments include PV cells with low reverse-breakdown characteristics, active bypass switches, and open-circuit protection system. The advantages and limitations of each approach will be discussed and compared to the proposed hot spot mitigation technique.

5.1   *Conventional Bypass Diodes*

Bypass diodes help to limit the maximum output power that can be dissipated through a reverse-biased PV cell, but the power level depends on the length of the cells in the PV module. More cells in the series PV module will dissipate more heat than strings with fewer cells [23 and 24]. Thus, bypass diodes are more effective in mitigating hot spots for short PV module length. For example, placing bypass diodes over every two cells would ensure that a PV cells never dissipate more than the nominal power of two cells, which is the required power that is unlikely to damage the cells [16].

The addition of discrete or integrated bypass diodes at the individual cell level increases the cost, therefore, this mitigation technique is prohibitively expensive such that individual bypass diodes have generally not been implemented and are unlikely to be adopted in the near future. Thus, other low-cost and practical hot spot protection method is needed.

5.2   *Active Bypass Switches*

When a bypass diode turn "on", it has a forward voltage that increases the voltage imposed on a hot spotting cell and it also dissipates additional power. Active switch solutions have been proposed by G. Acciari et al [25] that short the PV substring when it is bypassed, which have been also commercialized as "Smart bypass diodes" as in [26 and 27]. The active bypass switch method reduces the voltage over the PV string during bypass and the resulting power loss.

15

Active bypass switches are incrementally better for hot spot mitigation than bypass diodes. Table 4 shows the result after short circuiting a substring which has been affected by the hot spot, where the G and T is equal to 720 W/m^2 and 19 ^0C respectively. The results show that there is an improvement in the output power, however, it is not enough to prevent hot spotting.

The power loss is equal to 2.8 W using the active bypass switches method proposed by [25], however, the hot spot mitigation technique illustrated in this paper has only 0.7 W output power loss.

Table 4 Comparison between active bypass switches method and the proposed hot spot mitigation technique proposed in this research

	Before Considering hot spot mitigating technique	Hot spot mitigation technique proposed by [26]	Hot spot mitigation technique proposed in this paper
Theoretical Power (W)	181.5	181.5	181.5
Measured Power (W)	177.2	178.7	180.8
Power Loss (W)	4.3	2.8	0.7

6.   *Conclusion*

In this paper, the design and development of a hot spot mitigation technique is proposed. The proposed technique is capable to improve PV modules output power which are effected by hot spots. The suggested technique use two MOSFTEs, while the detection of hot spots was captured using FLIR i5 thermal imaging camera.

Several experiments conducted during various environmental conditions, where the PV module P-V curve was evaluated in each observed experiment, thus to analyse the output power performance with and without the proposed hot spot mitigation technique.

One PV module affected by a hot spot was tested. The output power increased approximately by 3.6 W after the activation of the hot spot mitigation technique. Additional test was examined while connecting the hot spot PV module in series with two other PV panels. The results indicate that there is 3.57 W increase in the output power after activating the hot spot protection technique.

In future, it is intended to improve the hot spot mitigation technique to work with several PV array configuration systems. In addition, the technique can be improved to enhance the output power of micro cracked PV modules.

7. *References*

[1] Blake, F. A., & Hanson, K. L. (1969, August). The hot-spot failure mode for solar arrays. In *Proceedings of the 4th Intersociety Energy Conversion Engineering Conference* (pp. 575-581).

[2] Dhimish, M., Holmes, V., Mehrdadi, B., Dales, M., Chong, B., & Zhang, L. (2017). Seven indicators variations for multiple PV array configurations under partial shading and faulty PV conditions. *Renewable Energy*.

[3] Orduz, R., Solórzano, J., Egido, M. Á., & Román, E. (2013). Analytical study and evaluation results of power optimizers for distributed power conditioning in photovoltaic arrays. *Progress in Photovoltaics: Research and Applications*, *21*(3), 359-373.

[4] Simon, M., & Meyer, E. L. (2010). Detection and analysis of hot-spot formation in solar cells. *Solar Energy Materials and Solar Cells*, *94*(2), 106-113.

[5] Chaturvedi, P., Hoex, B., & Walsh, T. M. (2013). Broken metal fingers in silicon wafer solar cells and PV modules. *Solar Energy Materials and Solar Cells*, *108*, 78-81.

[6] M. Dhimish, V. Holmes, B. Mehrdadi, M. Dales, The Impact of Cracks on Photovoltaic Power Performance, *Journal of Science: Advanced Materials and Devices* (2017), doi: 10.1016/j.jsamd.2017.05.005.

[7] Dhimish, M., Holmes, V., Mehrdadi, B., Dales, M., & Mather, P. (2017). Photovoltaic fault detection algorithm based on theoretical curves modelling and fuzzy classification system. *Energy*, *140*, 276-290.

[8] Moretón, R., Lorenzo, E., & Narvarte, L. (2015). Experimental observations on hot-spots and derived acceptance/rejection criteria. *Solar energy*, *118*, 28-40.

[9] Dhimish, M., Holmes, V., Mehrdadi, B., Dales, M., & Mather, P. (2017). Detecting Defective Bypass Diodes in Photovoltaic Modules using Mamdani Fuzzy Logic System. *Global Journal of Researches in Engineering: F Electrical and Electronics Engineering*, *17*(5), 33-44.

[10] Chen, K., Chen, D., Zhu, Y., & Shen, H. (2012). Study of crystalline silicon solar cells with integrated bypass diodes. *Science China Technological Sciences*, *55*(3), 594-599.

[11] Daliento, S., Mele, L., Bobeico, E., Lancellotti, L., & Morvillo, P. (2007). Analytical modelling and minority current measurements for the determination of the emitter surface recombination velocity in silicon solar cells. *Solar energy materials and solar cells*, *91*(8), 707-713.

[12] Dhimish, M., Holmes, V., Mehrdadi, B., & Dales, M. (2018). Comparing Mamdani Sugeno fuzzy logic and RBF ANN network for PV fault detection. *Renewable Energy*, *117*, 257-274.

[13]   Silvestre, S., Boronat, A., & Chouder, A. (2009). Study of bypass diodes configuration on PV modules. *Applied Energy*, *86*(9), 1632-1640.

[14]   Dhimish, M., Holmes, V., Mehrdadi, B., & Dales, M. (2017). Diagnostic method for photovoltaic systems based on six layer detection algorithm. *Electric Power Systems Research*, *151*, 26-39.

[15]   Coppola, M., Daliento, S., Guerriero, P., Lauria, D., & Napoli, E. (2012, June). On the design and the control of a coupled-inductors boost dc-ac converter for an individual PV panel. In *Power Electronics, Electrical Drives, Automation and Motion (SPEEDAM), 2012 International Symposium on* (pp. 1154-1159). IEEE.

[16]   Kim, K. A., & Krein, P. T. (2015). Reexamination of photovoltaic hot spotting to show inadequacy of the bypass diode. *IEEE Journal of Photovoltaics*, *5*(5), 1435-1441.

[17]   d'Alessandro, V., Guerriero, P., Daliento, S., & Gargiulo, M. (2011). A straightforward method to extract the shunt resistance of photovoltaic cells from current–voltage characteristics of mounted arrays. *Solid-State Electronics*, *63*(1), 130-136.

[18]   Daliento, S., Di Napoli, F., Guerriero, P., & d'Alessandro, V. (2016). A modified bypass circuit for improved hot spot reliability of solar panels subject to partial shading. *Solar Energy*, *134*, 211-218.

[19]   M. Dhimish, V. Holmes, M. Dales, Parallel fault detection algorithm for grid-connected photovoltaic plants, Renewable Energy (2017), doi: 10.1016/j.renene.2017.05.084.

[20]   Dhimish, M., Holmes, V., Mehrdadi, B., & Dales, M. (2017). Simultaneous fault detection algorithm for grid-connected photovoltaic plants. *IET Renewable Power Generation*, *11*(12), 1565-1575.

[21]   Simpson, L. (2009). The FLIR i5 Infrared Camera-Just aim and shoot to get a false-colour picture showing the temperature gradients of a building, machinery, a human body or whatever. And it can function as a precise non-contact thermometer. *Silicon Chip*, *22*(10), 12.

[22]   Solmetric. (2017). *PV Analyzer I-V Curve Tracers*. Retrieved from http://www.solmetric.com/pvanalyzermatrix.html.

[23]   Kim, K. A., Seo, G. S., Cho, B. H., & Krein, P. T. (2016). Photovoltaic hot-spot detection for solar panel substrings using ac parameter characterization. *IEEE Transactions on Power Electronics*, *31*(2), 1121-1130.

[24]   Dhimish, M., Holmes, V., Dales, M., & Mehrdadi, B. (2017). The effect of micro cracks on photovoltaic output power: case study based on real time long term data measurements. *Micro & Nano Letters*.

[25]   Acciari, G., Graci, D., & La Scala, A. (2011). Higher PV module efficiency by a novel CBS bypass. *IEEE transactions on power electronics*, *26*(5), 1333-1336.

[26]   *SM74611 Smart Bypass diode*, Datasheet, Texas Instruments, Dallas, TX, USA, 2013.

[27]   Zhang, M., & Kang, J. (2017). *U.S. Patent No. 9,541,598*. Washington, DC: U.S. Patent and Trademark Office.